Article

WetSpass-Based Study of the Effects of Urbanization on the Water Balance Components at Regional and Quadrat Scales in Beijing, China

Yueqiu Zhang, Shiliang Liu * iD, Fangyan Cheng and Zhenyao Shen

School of Environment, State Key Laboratory of Water Environment Simulation, Beijing Normal University, Beijing 100875, China; 13324103182@163.com (Y.Z.); 201531180030@mail.bnu.edu.cn (F.C.); z.y.shen@163.com (Z.S.)

*   Correspondence: shiliangliu@bnu.edu.cn

Abstract: China is the largest country in terms of population and its booming urbanization has exerted negative effects on ground-surface hydrological processes at different spatial scales, land-use types, and water balance, such as surface runoff, groundwater recharge, and evapotranspiration. However, it is not yet well understood as to how the modifications of the spatial patterns of landscapes affect the water balance on a regional scale. In this study, the water and energy transfer among soil, plants, and atmosphere (WetSpass) model was applied to evaluate the urbanization effects on the water balance on a regional scale by using Beijing as the case city for this current study. The relationships among impervious surfaces, landscape pattern indices, and water balance components were also quantified. Results indicated built-up land in 2012 was 673 km^2 larger than it in 2000, mostly converted from croplands. WetSpass model also indicated the variation rates of annual average surface runoff, evapotranspiration and groundwater recharge were 7%, 0.4% and −2% in the whole Beijing area, while they reached 52%, 6% and −24% in the urban area of Beijing from 2000 to 2012, respectively. At a city scale, four districts—Dongcheng, Xicheng, Chaoyang, and Haidian—were characterized by higher impervious percentage, as reflected by lower groundwater recharge and higher surface runoff than other districts. At quadrat scale, however, groundwater recharge (surface runoff) was negatively (positively) correlated with impervious percentages. For landscape indices, the Aggregation Index was positively correlated with surface runoff and negatively correlated with groundwater recharge while Patch Density Index, Splitting Index, Patch Richness Density Index, and Shannon's Diversity Index presented opposite relationships. The results of this study can help to develop human knowledge about the impacts of urbanization on hydrological cycles on a regional scale.

Keywords: urbanization; water balance; landscape index; hydrological model; Beijing

1. Introduction

Due to rapidly increasing population and developing economy, the urban area is expanding rapidly. As a result, the characteristics of urban hydrological cycle are being increasingly modified. Furthermore, the amounts, rates, locations and timing of water balance components, such as surface runoff, groundwater recharge and evapotranspiration, are making different responses worldwide [1]. In the process of urban expansion, the most important change is the increase of impervious surface, which will affect the groundwater level, interception, evaporation and consequently influence runoff, evapotranspiration and basic flow.

Groundwater recharge is vital for water supply of food production, agricultural irrigation and drinking water for most urban areas. Its sources and flow paths can be altered compared with the

natural conditions due to urbanization, which will cause a series of adverse effects on the surrounding environment [2]. Furthermore, the occurrence of large urban areas can change the runoff coefficient, flow direction, and base flow, and finally influence hydrological balance. In addition, the underlying surface changes due to urbanization will lead to a reduction in vegetation area, and hence decrease interception rate. Therefore, similar precipitation events will produce more ground-surface runoff on impervious surface than vegetated surfaces [3]. In addition, the total evapotranspiration, including vegetation transpiration and soil evaporation, which are complex and affected by land-use types, soil types, precipitation, and other environmental factors, will also decrease or increase because of increased impervious ground surfaces [4]. Therefore, rapid urban expansion has important effects on water balances and influences the management of water resources.

Large-scale urbanization and its effects on hydrological cycles and ecological environment on regional and global scales have been widely discussed in recent years [5,6]. Many have believed that urbanization can trigger a widespread transition from natural landscapes to man-made landscapes and greatly modify the types of land use and land cover and landscape characteristics [7]. Especially, the increases in impervious surfaces make the urban landscape patterns tend to be more fragmented and complex [8,9]. More importantly, changes in landscape patterns due to urban expansion can lead to a series of hydrological effects, such as the alteration of the underlying surface, total runoff volume, and flow characteristics of flood peak [10]. As a result, urban expansion can modify precipitation changes with respect to spatial patterns and precipitation quantities. These disastrous hydrological issues were usually considered as a kind of "urban disease" caused mainly by disturbed water balances and flood risks [11]. Specifically, land-use changes dominated by shifts from vegetated land to impervious surfaces could trigger occurrences of alterations of hydrological processes and hence disastrous hydrological extremes [12].

The hydrological effects of urbanization have been attracting more attention. Previous studies have mainly focused on the impacts of land-use and land-type variations on hydrographic features, such as the storm-water runoffs [13]. Corbett et al. [14] found a linear relationship between impervious surfaces and runoffs. The streamflow characteristics of a highly urbanized watershed in Atlanta area were compared with less urbanized and non-urbanized watersheds by Rose et al. (2001) [15], and the results indicated that the peak flows in the highly urbanized watersheds were 30% to 100% greater than those in the less urbanized watersheds. Grischek et al. (1996) [16] found the groundwater recharge in Dresden, Germany decreased by 23% due to impervious surface. However, many inconsistent results were also found in previous literatures. Kalin and Hantush [17] simulated the effects of land-use changes on hydrological characteristics, pointing out that the base flow would decrease with 31% magnitude when 60% of forested lands were translated into built-up lands. Barron et al. (2012) [18] pointed out that the groundwater recharge rates in Perth, Australia, were 2–3 times higher than those in less-urban conditions along with the lower evaporative losses. Therefore, the effects of urbanization on water balance components for different study areas were hard to predict due to human activities and natural factors.

A series of hydrological models have been developed to simulate and quantify the effects of urbanization on the hydrological effects [12]. Physically distributed models, such as MIKE SHE (System Hydrological European), have performed well in ungauged basins [19]. TOPMODEL (Topographic Hydrologic Model) is suitable for determining the areas of runoff in mountainous regions [20]. The SWAT (Soil and Water Assessment Tool) was applied widely to predict the effects of different soil textures, vegetation covers, and land-use on water production, sediment yield and non-point source pollution, which requires large and complicated parameters [21]. For researching the regional water balances, the WetSpass model is definitely the right choice [22]. It takes many influencing factors, such as land-use type, terrain, temperature, precipitation, and wind speed into account, and can quantify the long-term effects of urbanization on the water regime in a watershed. More importantly, it is customizable and adapts easily to new definitions of parameters [23,24].

In recent years, how land-use change has affected the hydrological cycle and hydrological components has been studied based on the WetSpass model worldwide. For example, Wang et al. (2012) [25], Gebreyohannes et al. (2013) [22] and Zomlot et al. (2015) [26] evaluated the spatial distribution of water resources, including groundwater recharge and runoff, based on WetSpass model. In addition, Zomlot et al. (2017) [27] assessed the importance of different controlling factors in groundwater recharge. WetSpass and GIS were used to study rainfall infiltration recharge under the influences of different land uses in the Songnen Basin in Northeast China [28]. Dams et al. (2013) [29] evaluated the hydrological dynamics using WetSpass and remote sensing techniques to interpret the impervious surface changes. Poelmans et al. (2010) [12] coupled three urban expansion scenarios with hydrological models and identified the importance of spatial pattern. However, little is known about the changes of specific hydrological components due to urbanization at different scales. Furthermore, applications of the WetSpass model with landscape dynamics assessments of the watersheds with rapid urban expansion are still lacking. In addition, the extent to which the changes in the landscape patterns affect the hydrological cycle has not yet been clarified. The clarifications of these scientific issues are of great scientific and theoretical merit in terms of the hydrological effects of urbanization and hydrological responses to human activities at different spatial and temporal scales.

Beijing, the largest city in China, has undergone remarkably rapid urbanization processes in recent decades. In the process of city development, the types of land use have changed greatly, and the hydrological cycle has experienced significant alterations. Some studies have shown that the groundwater level has declined rapidly in Beijing due to over-exploitation and decreased groundwater recharge [30]. In addition, the agricultural land area has decreased greatly. With rapid urbanization and an increased population, the shortage of water resources has become an important factor affecting the economic development of Beijing. It is therefore necessary to analyze how the water balance has changed due to urban expansion in the past decades at different scales and identify the relationship between landscape pattern and water balance components. The objectives of this study are to address the following scientific issues:

(1) How does urbanization impact the water balance components (groundwater recharge, surface runoff and evapotranspiration) at a city scale and a quadrat scale based on the WetSpass model?
(2) What are the relationships between impervious percentages and water balance?
(3) What are the relationship between landscape indices and groundwater recharge, surface runoff?

Answering these issues will enhance our understanding of the effects of urbanization on water balance and will provide an effective way to evaluate the relationships among impervious surface percentages, landscape index, and water balance.

2. Data and Methods

2.1. Study Area

Beijing is located in the North China Plain (39°28′–41°05′ N, 115°25′–117°30′ E), covering 14 districts and 2 counties with a total area of 16,410 km^2 [31]. The urban area is surrounded by high mountains in the western and northern sides with altitudes of 1000–1500 m. The plains area in Beijing covers 6390.3 km^2 in the eastern and southern parts of the Beijing metropolitan region [32]. Beijing has a warm temperate continental monsoon climate and the seasonal distribution of precipitation in this area is not even and the annual average precipitation has been about 600 mm in recent years, almost 80% of which is concentrated in summer (from June to September) [33]. The annual average temperature ranges 10 °C–12 °C, and the soil texture mainly consists of sand, loamy sand, sandy loam, silty loam, loam, sandy clay loam, clay loam, and clay [34]. In the past three decades, Beijing has been undergoing fast economic development and urban construction, and the urban population increased from 9.0 million to 23.0 million [35]. In addition, the city sprawls out following a share pie development model with a series of concentric ring roads construction. The study area is shown in Figure 1.
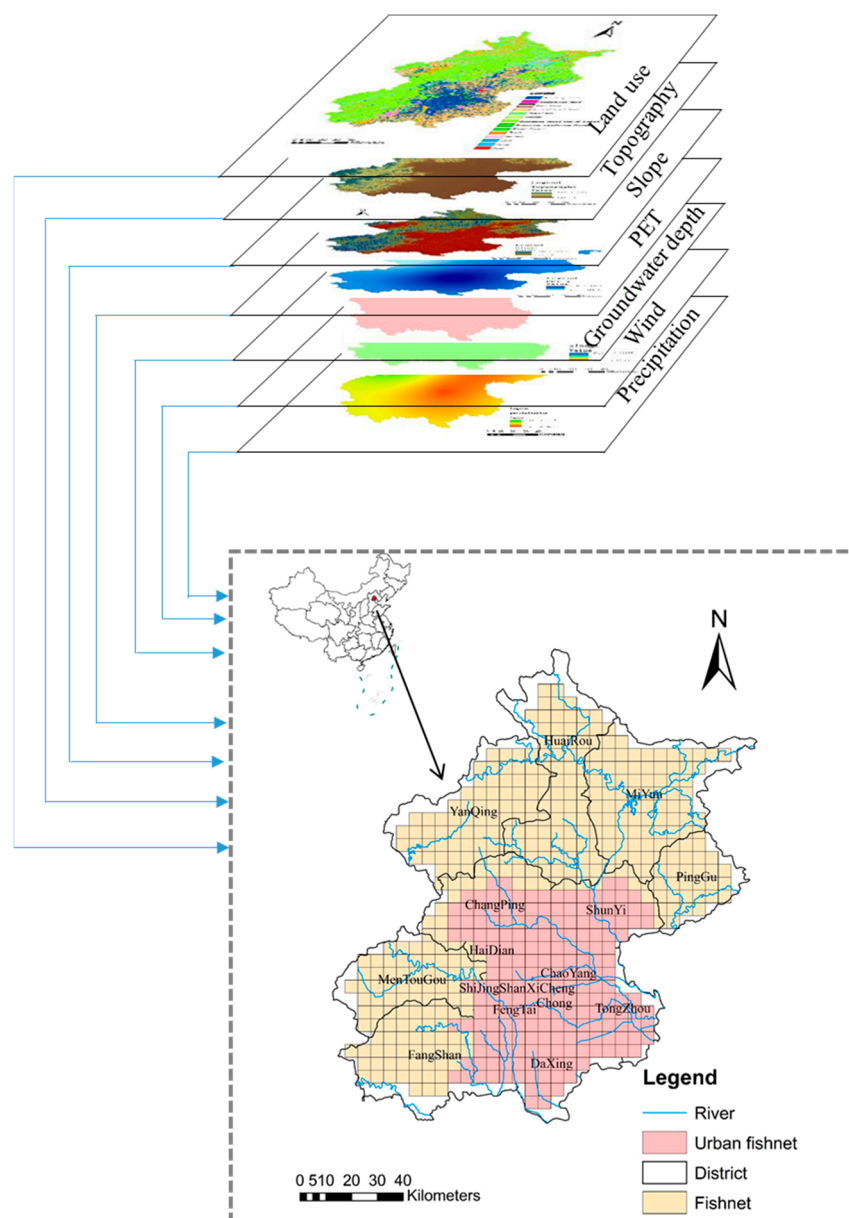
Figure 1. Location of the study area and the quadrat fishnet.

2.2. Data

WetSpass requires a combination of ArcView grid files, including land use, precipitation, potential evapotranspiration (PET), wind speed, topography, slope, soil texture, and groundwater depth (Figure 1). Land-use data, including for 2000 and 2012, were initially obtained from two Landsat TM images (Row 33, Path 123), both collected from June to September for the year with accuracy of the Kappa statistics of 0.89 and 0.84, respectively. A digital elevation model (DEM) with a resolution of 30 m is available in Global Land Cover Facility (http://gdem.ersdac.jspacesystems.or.jp/). Slope was derived by Spatial Analyst Tools with the GIS. The 1:1,000,000 soil texture data were initially obtained from the soil map provided by China Soil Database at (http://www.soil.csdb.cn/). Monthly data of precipitation and wind speed in 2000 and 2012 were derived from 20 local meteorological stations including Changping, Huairou, Miyun, Yanqing and elsewhere. Potential evapotranspiration (PET) was calculated by the Pennman-Monteinth equation. Twenty-seven groundwater depth data at point

level were referred to the *China Geological Environment Monitoring Groundwater Level Yearbook in 2000 and 2012*, and the spatial map of groundwater depth was derived by kriging interpolation.

2.3. Methods

2.3.1. GIS Analysis and Landscape Pattern Index Calculation

Landsat TM images were digitalized and interpreted to analyze impervious surfaces and landscape changes and their effects on hydrological characteristics. Based on supervised classifications and field survey data with current land-use maps, land-use types in Beijing are subdivided into the following 14 categories: built-up land, industrial land, bare land, agricultural land, grassland, meadow, deciduous broad-leaved forest, coniferous forest, mixed forest, shrub, wetland, lake, river, and road.

To study the relationship between impervious percentages and water balance, the impervious surfaces, mainly consisting of built-up land, industrial land and roads, were extracted. The impervious percentage can be considered as the proportion of those land-use types calculated by combining them together [36].

Urbanization always leads to changes in the landscape patterns. To better understand the relationship between landscape pattern and water balance, we attempted to study the variations of different landscape indices that could reflect landscape fragmentation and diversity information at different levels. Referring to the land-use change, human disturbance, and previous studies, we selected five typical landscape indices to quantify landscape pattern, including Patch Richness Density (PRD), Shannon's Diversity Index (SHDI), Patch Density (PD), Aggregation Index (AI), and Splitting Index (SPLIT) [37]. PRD and SPLIT were employed to quantify the fragmentation information. AI was used to assess the distribution of patch types. SHDI and PRD were used to quantify the structural components of the diversity information [38]. The above five indices, whose ecological meanings and mathematical expressions are shown in Table 1, were calculated by Fragstats 4.2 using the moving window analysis.

Table 1. Selected landscape indices and their ecological meanings.

Landscape Indices	Abbreviations	Formulas	Ecological Meanings
Patch Density	PD	$PD = N/A$	The larger the PD value, the more severe the degree of fragmentation.
Splitting Index	SPLIT	$SPLIT = \dfrac{A^2}{\sum\limits_{i=1}^{m}\sum\limits_{j=1}^{n} a_{ij}^2}$	The SPLIT value reflects the subdivision degree of a landscape.
Patch Richness Density	PRD	$PRD = m/A$	The PRD is larger if there are more patch types.
Shannon's Diversity Index	SHDI	$SHDI = -\sum\limits_{i=1}^{m} (P_i \times lnP_i)$	SHDI implies the abundance and distribution of different landscape types.
Aggregation Index	AI	$AI = \left(\sum\limits_{i=1}^{m} \left(\dfrac{g_{ii}}{max-g_{ii}} \right) P_i \right)$	AI increases with the more concentrated patch types.

Note: N = total number of patches in the landscape; A = total landscape area; a_{ij} = area of patch ij; m = number of patch types (classes) in the landscape; P_i = proportion of the landscape occupied by patch type (class) i; g_{ii} = number of like adjacencies (joins) between pixels of patch type (class) I; max-g_{ii} = maximum number of like adjacencies (joins) between pixels of patch type (class) i.

The research was conducted at city scale and quadrat scale, respectively. At quadrat scale, the continuous quadrats of 5 km × 5 km were delineated by ArcGIS to identify the correlations between impervious surface landscape patterns, and water balance at the quadrat scale. Totally, there are 5695 km × 5 km quadrats in the whole study area and only 201 quadrats in urban area of Beijing. The fishnet map is shown in Figure 1. In each quadrat, the average value of impervious percentages and different landscape pattern indices were calculated by zonal statistics in ArcGIS.

2.3.2. The WetSpass Model

WetSpass is a physically based, spatially distributed water balance model and can be used to simulate long-term annual and seasonal average surface runoff. Groundwater recharge and actual evapotranspiration on a regional scale can also be derived [39,40]. Inputs for this model contain several grid maps. Pre-defined parameters in the WetSpass model, including land use, soil types, and runoff coefficient, are connected to the model as attribute tables of their respective grids. The water balance is calculated for summer from April to September and winter from October to March. The results are consequently summed to obtain the annual values.

In this study, the grid size of raster data is 90 m × 90 m and the water balance computation is performed at a raster cell level. Water balance at each raster is obtained by summing the independent water balances for the vegetated, bare soil, open-water, and impervious fraction. The total water balance of a given area is thus calculated as the summation of the water balance of each raster cell. Taking the vegetated area as an example, the water balance can be calculated per grid according to Equations (1)–(3):

$$P = I + S_v + ET_v + R_v \tag{1}$$

$$ET_v = T_v + E_s \tag{2}$$

$$ET_{tot} = I + T_v + E_s \tag{3}$$

where P is the average annual precipitation (mm/year). I is the interception (mm/year) and depends on the vegetation types. S_v is the surface runoff (mm/year) related to precipitation amount, precipitation intensity, interception, and soil infiltration capacity. ET_v is the actual evapotranspiration (mm/year). R_v is the groundwater recharge (mm/year) calculated as a residual term of the water balance. The actual evapotranspiration, ET_v (mm/year), is the sum of T_v and E_s. The total actual evapotranspiration, ET_{tot} mm/year), is the sum of intersection (I), transpiration (T_v) and the evaporation, E_s (mm/year) from the bare soil. A similar procedure as that for the vegetated surfaces is followed for the calculation of bare-soil, open-water, and impervious surfaces. The only difference is that there is no vegetation in these cases and thus there is no interception and transpiration. A more detailed description, calibration, and validation of the WetSpass model can be found in Batelaan and Smedt (2007) [41].

2.3.3. Water Fluctuation Method

The correct calibration of a model can greatly improve its performance and hence the modelling results. To validate the performance of the optimized model after calibration, the water fluctuation method, which is widely applied to calculate the groundwater recharge, was also available to the calibration and validation of WetSpass model. The calculation formula is as Equation (4):

$$R_{\text{year}} = \mu \times \sum \Delta h \tag{4}$$

R_{year} is the yearly groundwater recharge (mm); μ represents the specific yield which is mostly relevant to lithology (Table 2); and $\sum \Delta h$ is the total variation amplitude of groundwater caused by precipitation.

Table 2. The empirical values of specific yield for different lithologies.

Lithology	μ	Lithology	μ
Clay	0.02–0.035	Medium sands	0.09–0.13
Loam	0.02–0.05	Medium coarse sand	0.10–0.15
Sandy loam	0.03–0.06	Coarse sand	0.11–0.15
Silty sand	0.06–0.1	Sandstone	0.02–0.03
Fine sand	0.08–0.12	Limestone	0.008–0.10

3. Results

3.1. The Impacts of Urban Expansion on Landscape Pattern

The comparison of two periods for land uses is shown in Figure 2. Overall, forests were widely distributed in the north and southwest parts and agricultural lands were relatively scattered. Grassland is mainly alpine meadow and distributed in the mountainous area. The proportion of bare land is very small and scattered. Built-up lands are in the center and southern part. Moreover, the built-ups areas increased and decentralized from 2000 to 2012. The transformed areas for each land-use type between 2000 and 2012 are presented in Figure 3.
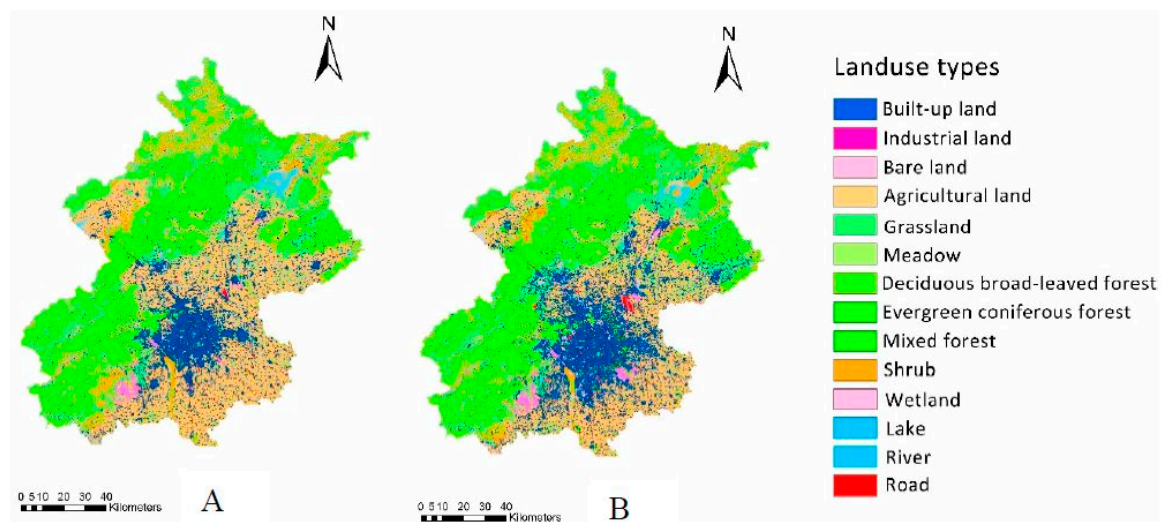

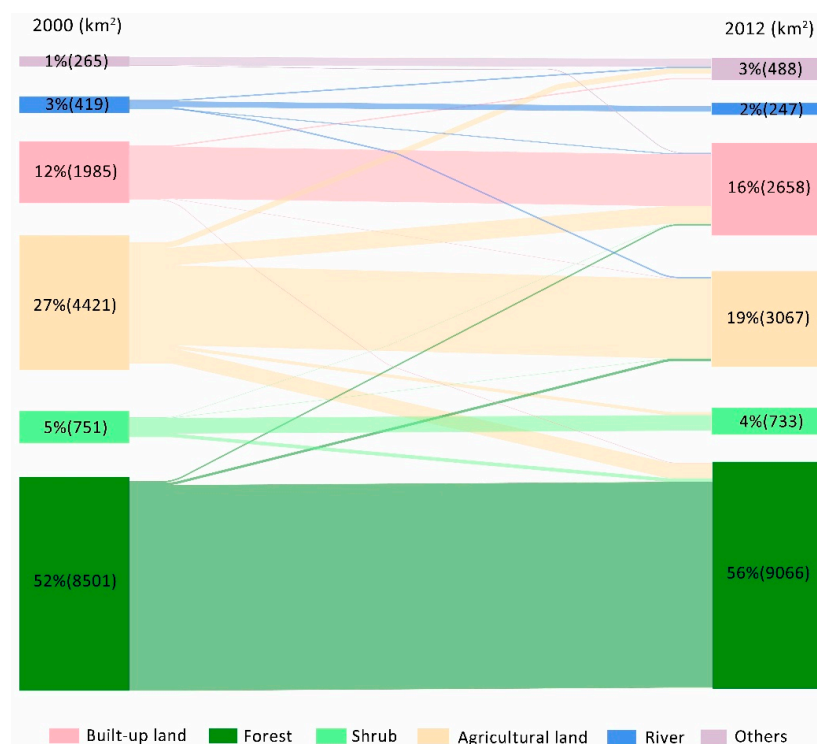**Figure 2.** The land uses in: 2000 (**A**); and 2012 (**B**).

Figure 3. Area change of different land-use types from 2000 to 2012.

As shown in Figure 3, forest is the largest land-use type in the area and composed of deciduous broad-leaved forest, evergreen coniferous forest, and mixed forest. In the past 13 years, the area of forests increased. In addition, agricultural land occupies a large area. From 2000 to 2012, the area of agricultural land declined greatly from 27% to 19% which was mostly converted into built-up land and mixed forest. City expansion resulted in the increase of built-up land and the amount in total reached 673 km^2 from 2000 to 2012. Specifically, 743 km^2 of built-up lands were translated from agricultural land (641 km^2), forest (49 km^2) and all other land use types (53 km^2), while total area of 80 km^2 for built-up lands were translated into agricultural land, grassland, forests, and roads.

From 2000 to 2012, the landscape indices were relatively stable but slightly increased as a whole (Table 3). PD was 0.28 higher in 2012 than 2000, which indicated that the degree of fragmentation increased due to urbanization and the result of SPLIT was consistent with PD. In addition, the larger AI value in 2012 showed the heterogeneity of the landscape increased. SHDI explaining the diversity of landscape increased when PRD increased, which suggested that the patches were more scattered.

Table 3. The landscape index of 2000 and 2012.

Landscape Index	2000	2012
Patch density	13.23	13.51
Splitting index	1.77	1.82
Aggregation index	87.63	87.52
Patch richness density	10.63	10.87
Shannon's Diversity Index	0.50	0.54

3.2. Simulation of Hydrological Distribution Based on WetSpass Model

3.2.1. The Calibration and Validation of WetSpass Model

In our simulation, three of the most sensitive input data were land-use parameter, soil parameter, and runoff coefficients. To obtain a best fit between observed and simulated water balance components, we constantly adjusted those parameters, combining actual investigation and related research [42,43].

As for land-use types, we should consider the runoff vegetation in the underlying surface, including grass, forest, crop, open water, and bare soil that were catalogued into vegetation, impervious area, open water, and bare land for each class according to the model's requirements (Table A1). In addition, the soil parameters consisted of field capacity, wilting point, plant available water content, residual water content, bare soil evapotranspiration depth, tension saturated height, and fraction of precipitation for summer and winter (Table A2). The accurate runoff coefficients for different land-use types, slopes, and soil types were crucial to the simulation of water balance components. In general, a higher slope would lead to higher runoff coefficients. With the same land-use type and slope, sand soil had the lowest runoff coefficient and clay soil had the highest. The specific parameters for land use, slope, and soil types are shown in Table A3.

The observed data were obtained from *China Groundwater Level Yearbook for Geo-Environmental Monitoring (2012)*, which recorded the detailed yearly groundwater levels from about 50 monitoring points in Beijing [44]. Among them, 23 monitoring points cannot be accurately positioned in Google Earth. To ensure the authenticity and accuracy of model verification, we chose the groundwater levels of 27 monitoring points to calculate the groundwater recharge as shown in Table A4. Furthermore, the simulated groundwater recharge at corresponding positions in 2012 were extracted by ArcGIS. Figure 4 displays the simulated and measured groundwater recharges, which showed a good linear relationship with an R^2 of 0.82. Thus, we assumed that the water balance components simulated by the WetSpass model in 2000 and 2012 are still reasonable.
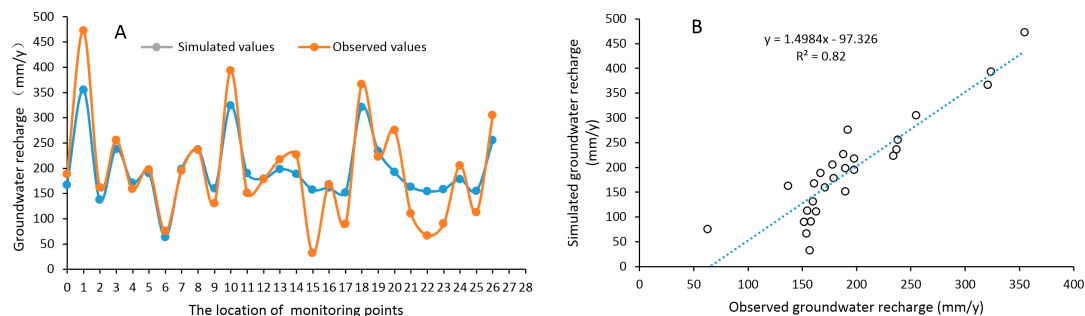
Figure 4. Evaluation of simulated and measured groundwater recharge: (**A**) the simulated values and observed values of groundwater recharge in 2012 for 27 monitoring points; and (**B**) the linear relationship between simulated and observed groundwater recharge.

3.2.2. The Water Balance Components of 2000 and 2012

Tables 4 and 5 show the seasonal and annual water balance components in the whole area of Beijing and only the urban region in Beijing for two periods. It is clear that the changing trends for each seasonal and annual water balance component were similar while the absolute values were different. Surface runoff and evapotranspiration both presented increasing trends while groundwater recharge decreased from 2000 to 2012. The annual average amount of precipitation was approximately 890 mm with 571 mm evapotranspiration, 277 mm recharge, and 43 mm runoff in 2000, while 573 mm evapotranspiration, 272 mm recharge, and 46 mm runoff in 2012.

Table 4. Seasonal and annual water balance components in the whole Beijing area from 2000 to 2012 (mm).

Parameter	Value	Runoff			Evapotranspiration			Recharge		
		Year	Winter	Summer	Year	Winter	Summer	Year	Winter	Summer
2000	Range	0–525	0–115	0–440	368–652	43–152	287–500	0–430	0–85	0–403
	Ave.	43	14	29	571	102	471	277	42	233
	SD	61	27	42	28	17	27	67	20	54
2012	Range	0–525	0–115	0–440	368–652	43–152	287–500	0–428	0–85	0–401
	Ave.	46	16	30	573	100	475	272	42	232
	SD	60	29	37	27	17	25	62	19	49
Variation $(\frac{Ave_{2012}-Ave_{2000}}{Ave_{2000}})$		+7%	+14.3%	+3%	+0.4%	+2%	+8%	−2%	0	−0.4%

Table 5. Seasonal and annual water balance components in urban region of Beijing from 2000 to 2012.

Parameter	Value	Runoff			Evapotranspiration			Recharge		
		Year	Winter	Summer	Year	Winter	Summer	Year	Winter	Summer
2000	Range	0–477	0–108	0–400	405–652	44–152	325–500	0–413	0–77	0–378
	Ave.	57	16	41	582	103	479	250	30	220
	SD	67	34	43	26	21	31	81	19	66
2012	Range	0–439	0–110	0–369	444–652	44–152	340–500	0–412	0–77	0–378
	Ave.	87	29	57	619	114	505	189	18	171
	SD	67	35	39	25	21	30	74	17	59
Variation $(\frac{Ave_{2012}-Ave_{2000}}{Ave_{2000}})$		+52%	+81%	+39%	+6%	+10%	+5%	−24%	−40%	−22%

In the whole Beijing region, the annual average surface runoff had the maximum variation rate, which reached 7%, while the variation rates for annual average evapotranspiration and groundwater recharge were less than 2% from 2000 to 2012. For different seasons, the amounts of water balance components in summer occupied a larger proportion than those in winter. However, the surface runoff

in winter varied greatly with increasing rate of 14.3% while the variation rate of evapotranspiration in summer increased by 8%.

In urban region in Beijing, the changing trends for water balance components were similar with those in the whole area. However, the variation rates from 2000 to 2012 were greatly different. The annual average surface runoff and evapotranspiration increased by 52% and 6%, respectively, while the annual average groundwater recharge decreased by 24%. In different seasons, the amounts and variation rates of surface runoff and evapotranspiration in urban region were both higher than those in the whole area while the groundwater recharge had the opposite state. The surface runoff increased by 81% and 39%, evapotranspiration increased by 10% and 5% while groundwater recharge decreased by 40% and 22% in winter and summer from 2000 to 2012, respectively.

3.3. Impacts of Urbanization on Water Balance Components

3.3.1. The Water Balance at Urban Scale

Spatially, the annual average runoff, groundwater recharge, and evapotranspiration indicated large heterogeneity for both 2000 and 2012. The range of higher surface runoff increased and the total evapotranspiration did not change greatly, as the groundwater recharge declined obviously according to the overlay of the layers in two periods. Furthermore, we found that the water balance is subject to a similar spatial pattern with that of districts, as shown in Figure 5.

Since the 1980s, the urban areas of Beijing have gradually expanded from the city center to nearby areas. The built-up area reached 1984 km^2 in 2000 and 2654 km^2 in 2012, according to the land-use reclassification of TM images and is mainly concentrated in Haidian, Chaoyang, Dongcheng, Xicheng, and other districts. Across the entire Beijing region, districts, including Xicheng, Dongcheng, Chaoyang, and Haidian, are characterized by lower groundwater recharge and higher surface runoff. However, suburban and rural areas are the opposite case, with Huairou, Yanqing, Fangshan, and Mentougou having higher groundwater recharge and lower surface runoff. From 2000 to 2012, Beijing underwent tremendous change in the land-use configuration as more districts were developed, especially Changping, Shunyi, and Tongzhou. Water balance varied due to urban expansion. We observed that areas of low groundwater recharge (red color) were scattered and had decreased, while the surface runoff increased considerably in 2012.

The variation in land-use types from 2000 to 2012 were considered as the main influencing factor to spatial differences of water balance components. To assess these influences, we compared the average annual recharge, surface runoff, and actual evapotranspiration for different land use types. The relationships between land use types and water balance components were relatively steady and existed little difference in the same area with short time interval. Figure 6 presents the water balance components as a result of different land cover types in 2000. Overall, the "high–low" sequence of recharge is bare land, grassland, shrub, agricultural land, and built-up land, successively. Furthermore, built-up land has the lowest groundwater recharge, except rivers and lakes, as the recharge from precipitation is very insignificant, and it has a relatively high surface runoff due to the ground with less roughness and higher impervious rates. As for forests, grasslands, and shrubs, they are characterized by a higher evapotranspiration and recharge when the runoff is reduced. In addition, the agricultural land and bare land have more ground-level low roughness ground-level, which leads to increased runoff and decreased evapotranspiration compared with built-up land. Therefore, land use types are considered as an important influencing factor in the dynamic of surface runoff, groundwater recharge, and actual evapotranspiration.
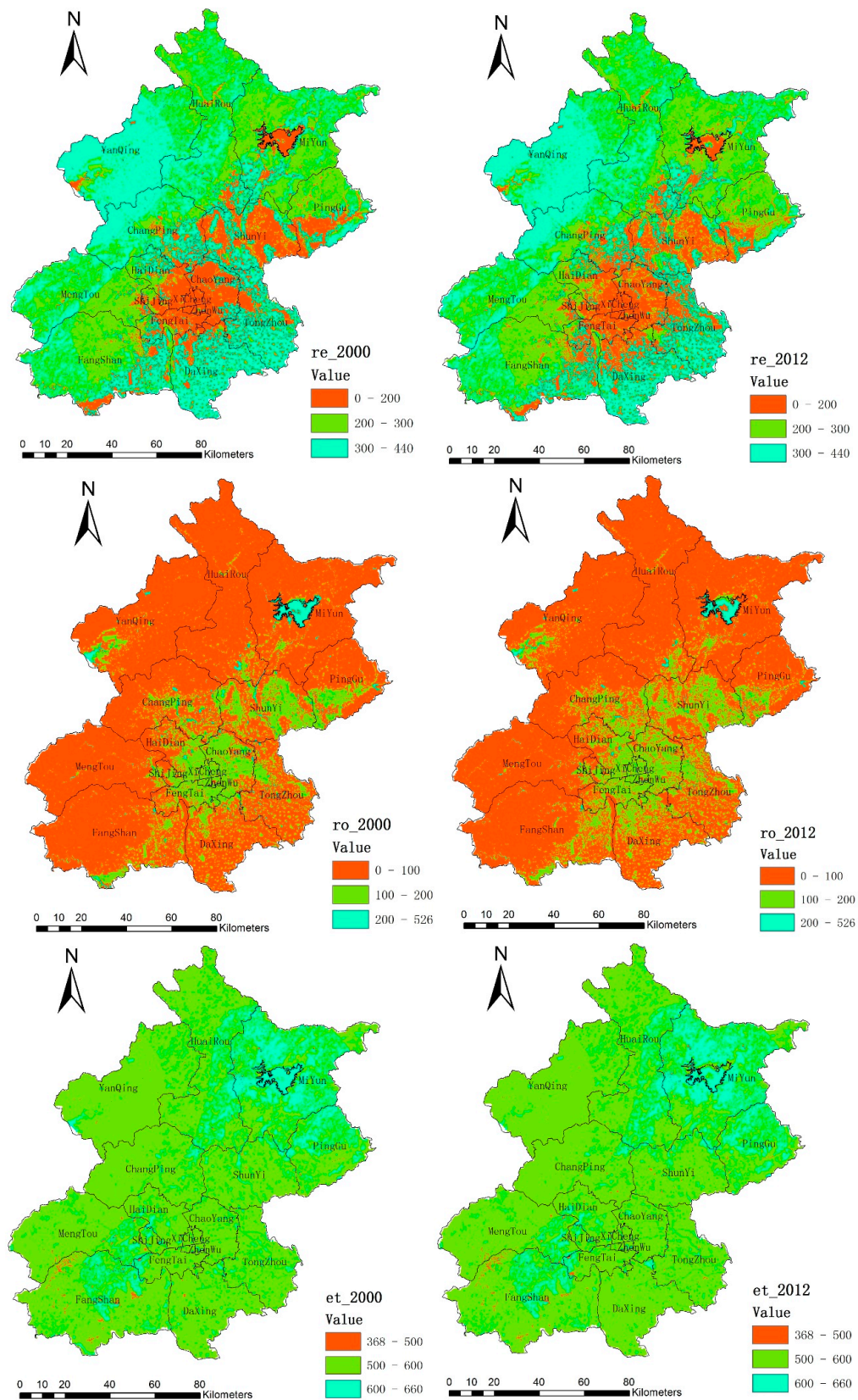
Figure 5. The water balance of 2000 and 2012 (re_2000, ro_2000 and et_2000 are groundwater recharge, surface runoff, and actual evapotranspiration for 2000, respectively; and re_2012, ro_2012 and et_2012 are groundwater recharge, surface runoff, and actual evapotranspiration for 2012, respectively).
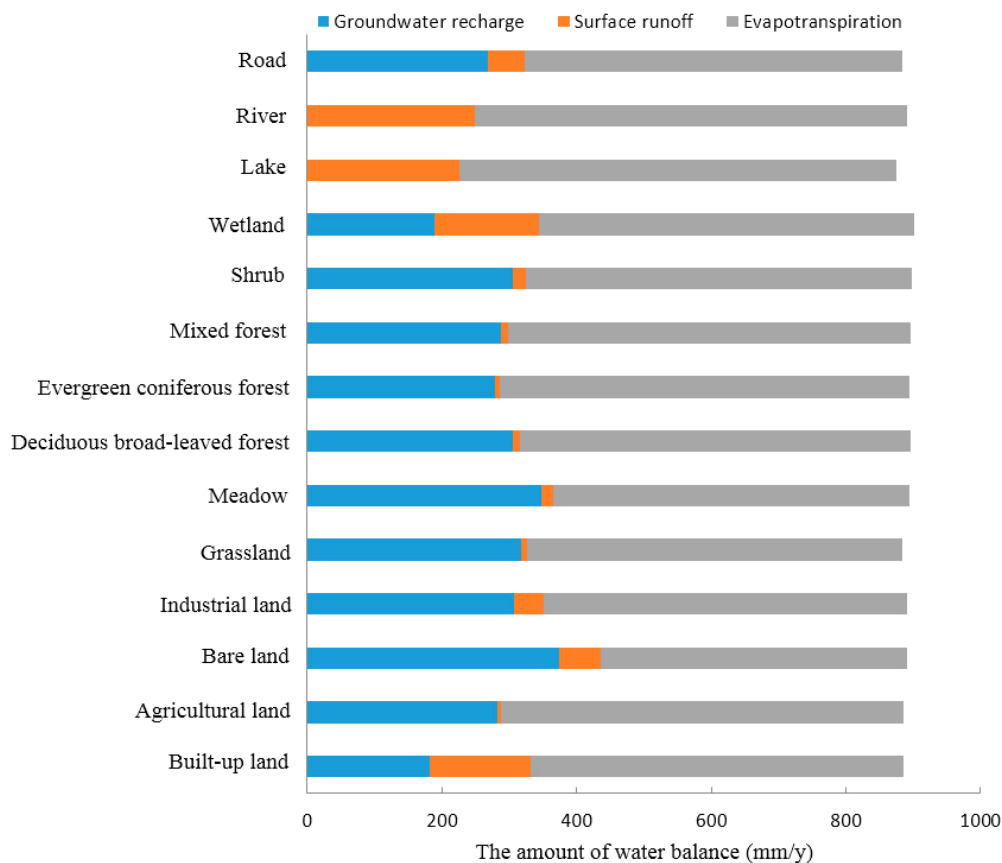
Figure 6. Average annual groundwater recharge, runoff and evapotranspiration for different land-use types.

3.3.2. The Impacts of Impervious Surface Percentages on Water Balance Components at Quadrat Scale

Urbanization level can be expressed as the impervious percentages to a certain extent. Higher impervious percentages imply larger areas of built-up land. On an urban scale, the impervious rate was 13.2% in 2000 and 16.3% in 2012. As the difference is relatively small to explain effectively the impacts on water balance on a regional scale, we analyzed the relationship between impervious percentages and water balance components at 5 km × 5 km quadrat scale. The impervious percentages in 569 quadrats can be assumed as an indicator of urban expansion because each quadrat has a consistent area and the water distribution can be compared. The simple linear regression models between the impervious percentages and water balance components in 2000 and 2012 are shown in Figure 7.

The results indicated that there was a significantly negative correlation between impervious percentages and groundwater recharge. The correlation coefficient, R^2, was 0.58 in 2000 and 0.65 in 2012, implying that the increased impervious percentages would lead to lower groundwater recharge. On the contrary, the impervious percentages positively correlated with surface runoff and the correlations were significant with the coefficients, with R^2 reaching 0.61 in 2000 and 0.65 in 2012, as shown in Figure 7A.

By comparison between 2000 and 2012, we found that 352 quadrats had higher impervious percentages in 2012 than 2000 due to urbanization in the whole area of Beijing. Among them, 336 quadrats had higher surface runoff, while 395 quadrats existed with a lower groundwater recharge in 2012 than 2000. However, in terms of evapotranspiration, it does not fit a linear relationship in the whole Beijing area. The main reason is we thought it might be attributed to the scale issue at the quadrat scale and there might be a threshold for the correlation when the whole study extent was taken into account. In our study, the cell size of land use types in 2000 and 2012 was 90 m × 90 m

and the cell size of the water balance study was 500 m × 500 m at quadrat scale. This resolution was suitable to characterize the urbanization in the whole Beijing area, while they may cause some errors for the relationship between imperious percentage and landscape configuration. Some research on urban ecology also verified that landscape configuration could affect heat island, evaporation and evapotranspiration.

To further understand the effects of urbanization on water balance components at quadrat scale, we extracted 201 quadrats in urban region in Beijing. We found surface runoff had significantly positive correlations while groundwater recharge had significantly negative correlations with impervious surface percentages both in 2000 and 2012. In addition, there existed positive, significant relationships between impervious surface percentage and evapotranspiration with correlation coefficient of 0.567 in 2000 ($p < 0.01$) and 0.510 in 2012 ($p < 0.01$), as shown in Figure 7B and Table 6.

(A)   **(B)**
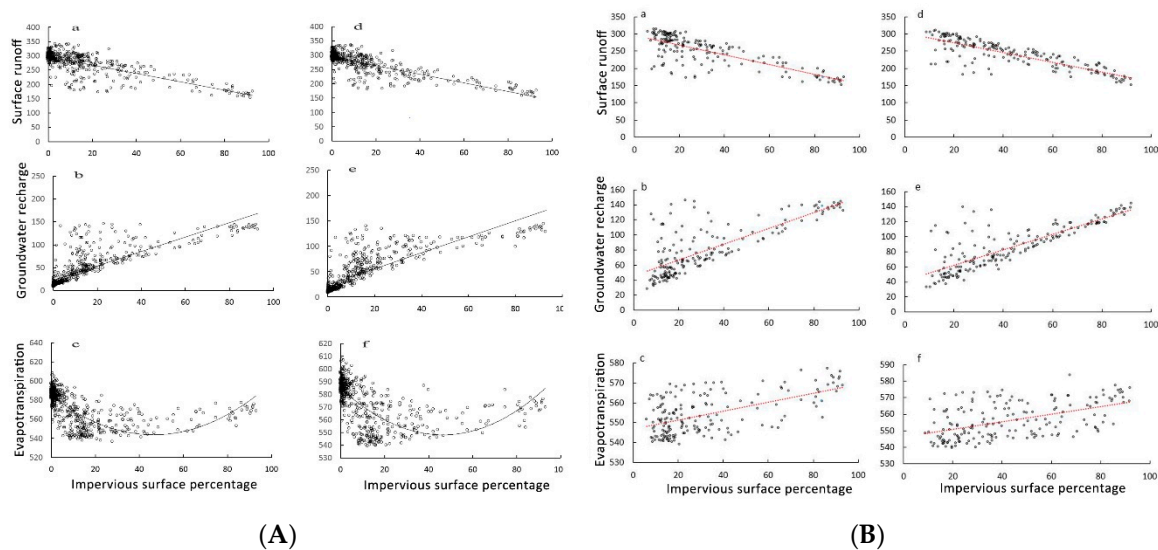
Figure 7. The correlations of groundwater recharge, surface runoff, and evapotranspiration with impervious percentages: in the whole Beijing area (**A**); and in urban region of Beijing (**B**) ((**a–c**) 2000; and (**d–f**) 2012).

Table 6. Correlations between the impervious percentages and water balance components in urban region of Beijing in 2000 and 2012.

Independent	Time	Dependent	Correlation model	R
Impervious percentages	2000	Groundwater recharge	$Y = -1.4241x + 296.28$	−0.769 **
		Surface runoff	$Y = 1.0454x + 45.985$	−0.783 **
		Evapotranspiration	$Y = 0.2261x + 546.8$	0.567 **
	2012	Groundwater recharge	$Y = -1.4205x + 303.52$	−0.834 **
		Surface runoff	$Y = 1.0241x + 41.671$	0.829 **
		Evapotranspiration	$Y = 0.2307x + 546.09$	0.510 **

Note: * significant at 0.05 level; ** significant at 0.01 level.

3.4. Relationship between Landscape Pattern Indices and Water Balance Components

In 2000 and 2012, the selected five landscape indices showed prominent correlations with groundwater recharge and surface runoff and the correlations decreased from 2000 to 2012. This can be seen in Figure 8. Specifically, AI has a remarkable positive correlation with surface runoff and a negative correlation with groundwater recharge, while the four other indices showed negative correlations with surface runoff and positive correlations with groundwater recharge. AI, SPLIT, and PD all reflect the scattered degree of the landscape. A decreased AI, and increased SPLIT and PD would result in decreased surface runoff and increased groundwater recharge. PRD and SHDI

revealed the landscape diversity, and increased PRD and SHDI should lead to decreased surface runoff and increased groundwater recharge.

Figure 8. The correlations between landscape index and groundwater recharge (re) and surface runoff (ro) (re-AI represents the correlation between groundwater recharge and AI; and ro-AI represents the correlation between surface runoff and AI).

4. Discussion

4.1. The Impacts of Urbanization on Water Balance

Land use will change during the process of urbanization and then disturb the natural water cycle. However, the water cycle processes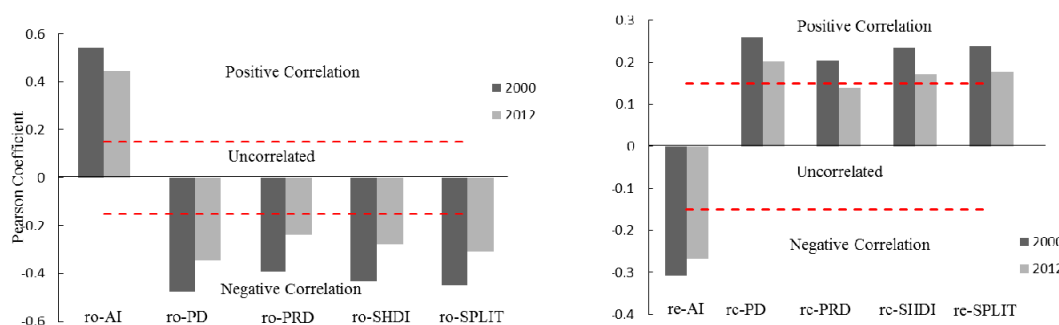 are difficult to estimate accurately and therefore there are many methods available such as the hydrology model method [45], remote sensing, the ArcGIS analysis method [46] and others. In our study, we used the WetSpass model to evaluate the changes of water balance components in the last 13 years, and comprehensively considered the influencing factors such as land-use types, topography, precipitation, and soil in this study. Each land-use type was a potential influencing factor behind the state of water bodies from hydrological pollution to distribution of water balance components [47]. Thus, studying the change of land-use types is important for explaining the effects of urbanization.

From 2000 to 2012, the built-up land increased 673 km^2 in Beijing, mostly converted from croplands. The result is consistent with Zhu et al. [48] as these researchers pointed out that the area of built-up land was three times higher in 1995 than 1982, after being converted from agricultural land and forests. Impervious surfaces such as built-up lands and other roads are the driving factor of hydrological changes because of urbanization [49].

It will be significant to quantify the water balance components responding to different land-use types, especially in built-up lands. Zomlot et al. [26] displayed how the built-up land had a lower groundwater recharge because of partially impervious surfaces, but the water distribution differed slightly in the average yearly evapotranspiration, groundwater recharge, and surface runoff at 450 mm, 235 mm, and 73 mm, respectively.

At the urban scale, districts, including Xicheng, Dongcheng, Chaoyang, and Haidian, are characterized by lower groundwater recharge (0–200 mm/year) and higher surface runoff (100–200 mm/year) than the suburban region including Huairou, Yanqing, Fangshan, and Mentougou (groundwater recharge of 200–400 mm/year and surface runoff of 0–100 mm/year). This is due to the gathered large-area land of built-up, traffic roads, and industrial land. The suburban area and country have an opposite case with wider natural land areas and fewer build up areas than urban locations. Pan et al. [34] and Zhu et al. [48] pointed that increased built-up lands in four districts of the city led to the variations of surface environment of the soil, which enlarged the areas of impervious surfaces.

However, no reports are available to address the impacts of urbanization on water balance on a quadrat scale. There was a significantly negative correlation between impervious percentages and groundwater recharge, and a positive correlation between impervious percentages and runoff both in 2000 and in 2012. Our results indicate that the correlation coefficient increased over time, which implied

that the increased impervious percentages would play a more important role in water distribution due to urbanization in Beijing.

In the process of urbanization, it is true the precipitation or drought at different scales, even the extreme weather, can affect the water balance at different scales components greatly. Therefore, it is better to consider the effects of climate change on hydrology. Globally, some previous studies distinguished the effects of climate change and urbanization on watershed hydrology [50–53]. It is noted that the climate change should be considered at a relatively longer time scale. In our study, the study period is from 2000 to 2012. In this period, the urban expansion in Beijing was very rapid and obvious. Comparatively, the variations of average annual precipitation are not distinct in the past decades although there could be extreme weather in some years (http://data.cma.cn/data/cdcindex).

In Beijing, many studies explored the relationships between rainfall storm flow and runoff to provide support for scientific decision to solve water management [54]. In addition, some studies in Beijing showed the effects of climate change and urbanization on groundwater recharge [55]. Studies indicated landscape pattern change, due to anthropogenic activities in the process of urbanization, played a major role to groundwater recharge [1,48]. In our study, we also attempted to establish the relationship between landscape pattern changes due to urbanization and the water balance components. Thus, we used the WetSpass which is a quasi-steady state spatially distributed water balance model to exhibit the relationship at different scales. Therefore, in this study, the precipitation dynamics was not the focus and we used the similar precipitation scenarios in two periods to analyze the effects of urbanization on water balance components as our study is a medium time scale research. In our future study, the process-based model WetSpa extension will be used considering the climate change and landscape variations as the influencing factors.

In addition, it is equally vital to consider the population and its influence on groundwater recharge. However, our study was mainly focused on the area of urbanization. As the area of urbanization and population is closely related, and these two factors can produce a doubled influence on groundwater recharge, we only considered the urbanization rate in area. The increased population and the associated potential effect on groundwater should be explored in future studies.

4.2. The Impacts of Landscape Indices on Water Balance

Landscape patterns can be easily quantified by different landscape indices such as area, edge, shape, aggregation, and diversity aspects [38]. Meanwhile, the landscape index could concentrate on the landscape information, reflecting the composition of the structural, spatial configuration that links landscape patterns and ecological process. Nowadays, landscape indices metrics are widely used in quantifying the composition and configuration of city expansion and dynamics [56]. Some findings indicated that Patch Density, Aggregation Index, and Splitting Index were sensitive to the different water-quality parameters [57]. However, these studies did not focus on the change of water balance based on the influence of variation of landscape pattern. In our study, we clarified how landscape pattern impacted the water quantity (groundwater recharge and surface runoff). Overall, PD, SPLIT, PRD, and SHDI increased slightly, while AI decreased from 2000 to 2012. The natural landscape, without human disturbance, usually has high AI, low SPLIT and PD, and high vegetation coverage and a large patch. However, along the gradient from outer suburban to urban, with increasing human disturbance, especially impervious surface, the original landscape pattern and underlying surface conditions will be modified. The scattered patches will lead to lower AI and higher SPLIT and PD values, and thus change flow regimes such as runoff directions and rates, and increase the annual runoff [58].

To clarify the influential process of landscape indices and water balance, we sampled the pixels of landscape indices and water balance components layers. These quadrats in Beijing were catalogued into four gradients: outer suburban, suburban, suburban transition zone and urban center. The variations of five landscape indices and water balance at different gradients were analyzed (Figure 9). We observed that PD, SPLIT, PRD, and SHDI generally decreased from outer suburban to urban center with

fluctuations in suburban transition zone, which had similar tendencies with groundwater recharge. In addition, AI tended to increase with a minimum value in suburban transition zone that had a similar tendency with surface runoff. The special reasons for the differences of landscape indices in outer suburban, suburban, suburban transition zone, and urban area will be studied deeply in future.
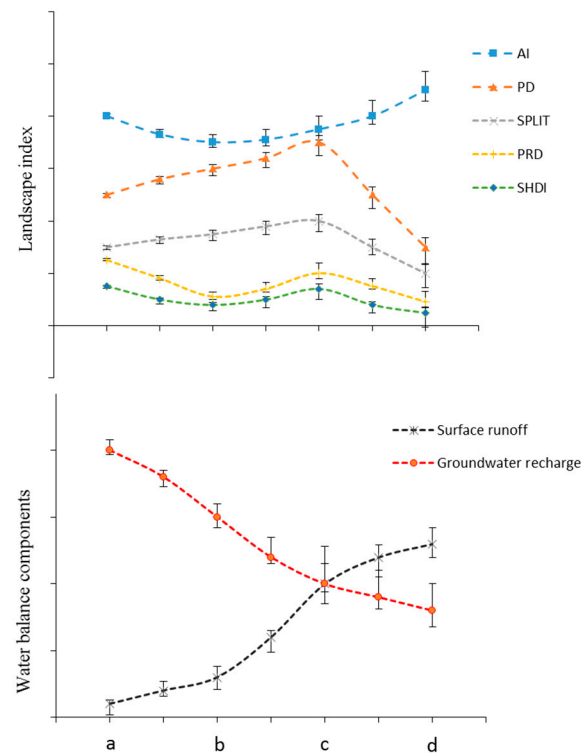
Figure 9. The changing trend of landscape indices and water balance components at four gradients: (**a**) outer suburban; (**b**) suburban; (**c**) suburban transition zone; and (**d**) urban center.

However, pattern indices alone may not be sufficient to display the whole city landscape changes, so we introduced the impervious percentage and carried out the research at different scales to obtain the quantitative relationships among landscape indices, impervious percentages and water balance components. Previous studies indicated that the urban green spaces, as a measure to reduce surface runoff and alleviate the negative effects on the hydrology in the process of urbanization, have attracted more attention [19]. In addition, for Beijing, the role of urban wetlands has gradually received great attention from urban planners and managers. Wetlands can be identified as natural sponges that would mitigate surface runoff, precipitation, snowmelt, and flood risks [59].

Thus, it will be necessary to increase the green lands, decrease impervious percentages for Beijing and plan the landscape pattern for different districts. Those results are meaningful for the management and spatial planning policymakers in the future.

5. Conclusions

In this paper, we mainly studied the effects of urbanization on water balance components and the correlations among water balance components, landscape index, and impervious percentages. The results of the WetSpass model showed that there are significant seasonal differences in surface runoff, groundwater recharge, and evapotranspiration. There was also a clear relationship between land use and water cycle, according to the spatial analysis of different locations. Built-up land and roads resulted in high surface runoff and low groundwater recharge while forests, shrubs, and grassland had the opposite situation. Combining the results of WetSpass in different districts, we found Xicheng, Dongcheng, Haidian, Chaoyang, and other districts where urbanization levels were relatively

higher had an increasing trend of runoff and a decreased trend of recharge. Moreover, the ranges of higher runoff and lower recharge region have been extended following the urban expansion direction. At quadrat scale, the results of correlation analysis between impervious percentages and hydrological characteristics indicated that impervious percentages and surface runoff presented a decreasing trend when impervious percentages and groundwater recharge displayed an increasing trend. When we studied the effects of landscape pattern on water balance components, we found that AI was positively correlated with surface runoff and negatively with groundwater recharge. PD, PRD, SPLIT, and SHDI were negatively correlated with surface runoff and positively with groundwater recharge.

In conclusion, urbanization changes the land-use type and increases the area of built-up land. As a result, the underlying surface varied, impervious areas increased, and the landscape pattern experienced changes. Finally, the water cycle process was influenced and water balances responded.

Author Contributions: Yueqiu Zhang and Shiliang Liu conceived and designed the experiments; Yueqiu Zhang performed the experiments and analyzed the data; Fangyan Cheng and Zhenyao Shen contributed reagents/materials/analysis tools; and Yueqiu Zhang wrote the paper.

Appendix A

Table A1. WetSpass land use parameter.

NUMBER ER	LUSE_TYPE	RUNOFF_VEG	NUM_VEG_RO	NUM_IMP_RO	VEG_AREA	BARE_AREA	IMP_AREA	OPENW_AREA	ROOT_DEPTH	LAI	MIN_STOM	INTERC_PER	VEG_HEIGHT
1	Build-up land	grass	2.00	1.00	0.20	0.00	0.80	0.00	0.30	2.00	100.00	10.00	0.12
2	Industural land	grass	2.00	9.00	0.40	0.00	0.60	0.00	0.30	2.00	100.00	10.00	0.12
3	Bare land	bare soil	4.00	0.00	0.00	1.00	0.00	0.00	0.05	0.00	110.00	0.00	0.00
4	Agriculture land	crop	1.00	0.00	0.00	1.00	0.00	0.00	0.35	0.00	180.00	0.00	0.60
5	Meadow	grass	2.00	0.00	1.00	0.00	0.00	0.00	0.30	2.00	100.00	10.00	0.20
6	Wet meadow	grass	2.00	0.00	1.00	0.00	0.00	0.00	0.30	2.00	100.00	10.00	0.30
7	Deciduous broad- leaved	forest	3.00	0.00	0.20	0.80	0.00	0.00	2.00	0.00	250.00	10.00	18.00
8	Evergreen coniferous forest	forest	3.00	0.00	0.90	0.10	0.00	0.00	2.00	4.50	500.00	45.00	15.00
9	Mixed forest	forest	3.00	0.00	0.50	0.50	0.00	0.00	2.00	4.50	500.00	38.00	15.00
10	Shrub	grass	2.00	0.00	0.20	0.80	0.00	0.00	0.60	0.00	110.00	5.00	2.00
11	Wetland	open water	5.00	0.00	0.40	0.20	0.00	0.40	0.30	2.00	110.00	10.00	0.50
12	Lake	open water	5.00	0.00	0.00	0.00	0.00	1.00	0.05	0.00	110.00	0.00	0.00
13	River	open water	5.00	0.00	0.00	0.00	0.00	1.00	0.05	0.00	110.00	0.00	0.00
14	Road	grass	2.00	5.00	0.60	0.10	0.30	0.00	0.30	2.00	100.00	10.00	0.12

Note: LUSE_TYPE: Land Use Type; RUNOFF_VEG: Runoff Vegetation; NUM_VEG_RO: Runoff class for vegetation type; NUM_IMP_RO: Imprevious Runoff class for impervious area types; VEG_AREA: Vegetated Area; BARE_AREA: Bare Area; IMP_AREA: Impervious Area; OPENW_AREA: Open-water Area; ROOT_DEPTH: Root depth; LAI: Leaf Area Index; MIN_STOM: Minimum Stomatal Opening; INTERC_PER: Interception Percentage; VEG_HEIGHT: Vegetation Height.

Table A2. WetSpass soil parameter.

NUMBER	SOIL	FIELDCAPAC	WILTINGPNT	PAW	RESIDUALWC	A1	EVAPODEPTH	TENSIONHHT	P_FRAC_SUM	P_FRAC_WIN
1	sand	0.12	0.05	0.07	0.020	0.51	0.05	0.07	0.09	0.01
2	loamy sand	0.15	0.07	0.08	0.035	0.47	0.05	0.09	0.09	0.01
3	sandy loam	0.21	0.09	0.12	0.041	0.44	0.05	0.15	0.09	0.01
4	silty loam	0.29	0.10	0.19	0.015	0.40	0.05	0.21	0.26	0.07
5	loam	0.25	0.12	0.13	0.027	0.37	0.05	0.11	0.15	0.02
6	sandy clayl	0.26	0.16	0.10	0.068	0.32	0.05	0.28	0.54	0.30
7	clayloa m	0.33	0.19	0.14	0.075	0.27	0.05	0.26	0.62	0.41
8	clay	0.46	0.33	0.13	0.090	0.21	0.05	0.37	0.95	0.85

Note: NUMBER: Soil type number; SOIL: Soil type (texture); FIELDCAPAC: Field capacity; WILTINGPNT: Wilting Point; PAW: Plant available water content; RESIDUALWC: Residual water content; A1: Calibration parameter dependent on the sand content of the soil; EVAPODEPTH: Bare soil evaporation depth; TENSIONHHT: Tension saturated height; P_FRAC_SUM: Fraction of summer precipitaion contributing to Hortonian runoff; P_FRAC_WIN: Fraction of winter precipitaion contributing to Hortonian runoff.

Table A3. Runoff coefficient parameters for vegetated, bare soil and open water raster cells.

LANDUSERO	LANDUSENUM	SLOPE_[%]	SLOPENUM	SOILTYPE	SOILNUM	RUNOFFCOEF	UNIQUE_NUM	SOIL_BARE	SLOPE_BARE	BAREROCOEF	UNIQUEBARE	NUM_IMP_RO	SLOPE_IMP	IMPROCOEF	UNIQUEIMP
crop	1	<0.5	1	sand	1	0.3500	111	1	1	0.4500	11	1	1	0.50	11
crop	1	0.5–5	2	sand	1	0.4000	112	1	2	0.4800	12	1	2	0.60	12
crop	1	5–10	3	sand	1	0.4500	113	1	3	0.5300	13	1	3	0.70	13
crop	1	>10	4	sand	1	0.5000	114	1	4	0.5800	14	1	4	0.80	14
grass	2	<0.5	1	sand	1	0.1500	121	2	1	0.4800	21	2	1	0.40	21
grass	2	0.5–5	2	sand	1	0.2000	122	2	2	0.5300	22	2	2	0.50	22
grass	2	5–10	3	sand	1	0.2500	123	2	3	0.5800	23	2	3	0.60	23
grass	2	>10	4	sand	1	0.3000	124	2	4	0.6300	24	2	4	0.70	24
forest	3	<0.5	1	sand	1	0.0500	131	3	1	0.5000	31	3	1	0.30	31
forest	3	0.5–5	2	sand	1	0.1000	132	3	2	0.5500	32	3	2	0.40	32
forest	3	5–10	3	sand	1	0.1500	133	3	3	0.6000	33	3	3	0.50	33
forest	3	>10	4	sand	1	0.2000	134	3	4	0.6500	34	3	4	0.60	34
bare soil	4	<0.5	1	sand	1	0.4500	141	4	1	0.5300	41	4	1	0.30	41
bare soil	4	0.5–5	2	sand	1	0.4800	142	4	2	0.5800	42	4	2	0.40	42
bare soil	4	5–10	3	sand	1	0.5300	143	4	3	0.6300	43	4	3	0.50	43
bare soil	4	>10	4	sand	1	0.5800	144	4	4	0.6800	44	4	4	0.60	44
openwater	5	<0.5	1	sand	1	1.0000	151	5	1	0.5000	51	5	1	0.30	51
openwater	5	0.5–5	2	sand	1	1.0000	152	5	2	0.5500	52	5	2	0.40	52
openwater	5	5–10	3	sand	1	1.0000	153	5	3	0.6000	53	5	3	0.50	53
openwater	5	>10	4	sand	1	1.0000	154	5	4	0.6500	54	5	4	0.60	54
crop	1	<0.5	1	Loamy-sand	2	0.3800	211	6	1	0.4800	61	6	1	0.30	61
crop	1	0.5–5	2	loamy-sand	2	0.4300	212	6	2	0.5300	62	6	2	0.40	62
crop	1	5–10	3	loamy-sand	2	0.4800	213	6	3	0.5800	63	6	3	0.50	63
crop	1	>10	4	loamy-sand	2	0.5300	214	6	4	0.6300	64	6	4	0.60	64
grass	2	<0.5	1	loamy-sand	2	0.1800	221	7	1	0.5300	71	7	1	0.30	71
grass	2	0.5–5	2	loamy-sand	2	0.2300	222	7	2	0.5800	72	7	2	0.40	72
grass	2	5–10	3	loamy-sand	2	0.2800	223	7	3	0.6300	73	7	3	0.50	73
grass	2	>10	4	loamy-sand	2	0.3300	224	7	4	0.6800	74	7	4	0.60	74
forest	3	<0.5	1	loamy-sand	2	0.0800	231	8	1	0.5500	81	8	1	0.50	81
forest	3	0.5–5	2	loamy-sand	2	0.1300	232	8	2	0.5800	82	8	2	0.60	82
forest	3	5–10	3	loamy-sand	2	0.1800	233	8	3	0.6300	83	8	3	0.70	83
forest	3	>10	4	loamy-sand	2	0.2300	234	8	4	0.6800	84	8	4	0.80	84
bare soil	4	<0.5	1	loamy-sand	2	0.4800	241	9	1	0.5800	91	9	1	0.30	91
bare soil	4	0.5–5	2	loamy-sand	2	0.5300	242	9	2	0.6300	92	9	2	0.40	92
bare soil	4	5–10	3	loamy-sand	2	0.5800	243	9	3	0.6800	93	9	3	0.50	93
bare soil	4	>10	4	loamy-sand	2	0.6300	244	9	4	0.7300	94	9	4	0.60	94
openwater	5	<0.5	1	loamy-sand	2	1.0000	251	10	1	0.6000	101			0.00	
openwater	5	0.5–5	2	loamy-sand	2	1.0000	252	10	2	0.6500	102			0.00	
openwater	5	5–10	3	loamy-sand	2	1.0000	253	10	3	0.7000	103			0.00	
openwater	5	>10	4	loamy-sand	2	1.0000	254	10	4	0.7500	104			0.00	
crop	1	<0.5	1	sandy-loam	3	0.4000	311	11	1	0.6300	111			0.00	
crop	1	0.5–5	2	sandy-loam	3	0.4500	312	11	2	0.6800	112			0.00	
crop	1	5–10	3	sandy-loam	3	0.5000	313	11	3	0.7300	113			0.00	
crop	1	>10	4	sandy-loam	3	0.5500	314	11	4	0.7800	114			0.00	
grass	2	<0.5	1	sandy-loam	3	0.2000	321	12	1	0.6500	121			0.00	
grass	2	0.5–5	2	sandy-loam	3	0.2500	322	12	2	0.7000	122			0.00	
grass	2	5–10	3	sandy-loam	3	0.3000	323	12	3	0.7500	123			0.00	
grass	2	>10	4	sandy-loam	3	0.3500	324	12	4	0.8000	124			0.00	
forest	3	<0.5	1	sandy-loam	3	0.1000	331			0.0000				0.00	
forest	3	0.5–5	2	sandy-loam	3	0.1500	332			0.0000				0.00	
forest	3	5–10	3	sandy-loam	3	0.2000	333			0.0000				0.00	
forest	3	>10	4	sandy-loam	3	0.2500	334			0.0000				0.00	
bare soil	4	<0.5	1	sandy-loam	3	0.5000	341			0.0000				0.00	
bare soil	4	0.5–5	2	Sandy-loam	3	0.5500	342			0.0000				0.00	
bare soil	4	5–10	3	sandy-loam	3	0.6000	343	0.0000	0.00						
bare soil	4	>10	4	sandy-loam	3	0.6500	344	0.0000	0.00						
openwater	5	<0.5	1	sandy-loam	3	1.0000	351	0.0000	0.00						
openwater	5	0.5–5	2	sandy-loam	3	1.0000	352	0.0000	0.00						
openwater	5	5–10	3	sandy-loam	3	1.0000	353	0.0000	0.00						
openwater	5	>10	4	sandy-loam	3	1.0000	354	0.0000	0.00						

Table A3. *Cont.*

LANDUSERO	LANDUSENUM	SLOPE_[%]	SLOPENUM	SOILTYPE	SOILNUM	RUNOFFCOEF	UNIQUE_NUM	SOIL_BARE	SLOPE_BARE	BAREROCOEF	UNIQUEBARE	NUM_IMP_RO	SLOPE_IMP	IMPROCOEF	UNIQUEIMP
crop	1	<0.5	1	silty-loam	4	0.4300	411	0.0000	0.00						
crop	1	0.5–5	2	silty-loam	4	0.4800	412	0.0000	0.00						
crop	1	5–10	3	silty-loam	4	0.5300	413	0.0000	0.00						
crop	1	>10	4	silty-loam	4	0.5800	414	0.0000	0.00						
grass	2	<0.5	1	silty-loam	4	0.2300	421	0.0000	0.00						
grass	2	0.5–5	2	silty-loam	4	0.2800	422	0.0000	0.00						
grass	2	5–10	3	silty-loam	4	0.3300	423	0.0000	0.00						
grass	2	>10	4	silty-loam	4	0.3800	424	0.0000	0.00						
forest	3	<0.5	1	silty-loam	4	0.1300	431	0.0000	0.00						
forest	3	0.5–5	2	silty-loam	4	0.1800	432	0.0000	0.00						
forest	3	5–10	3	silty-loam	4	0.2300	433	0.0000	0.00						
forest	3	>10	4	silty-loam	4	0.2800	434	0.0000	0.00						
bare soil	4	<0.5	1	silty-loam	4	0.5300	441	0.0000	0.00						
bare soil	4	0.5–5	2	silty-loam	4	0.5800	442	0.0000	0.00						
bare soil	4	5–10	3	silty-loam	4	0.6300	443	0.0000	0.00						
bare soil	4	>10	4	silty-loam	4	0.6800	444	0.0000	0.00						
openwater	5	<0.5	1	silty-loam	4	1.0000	451	0.0000	0.00						
openwater	5	0.5–5	2	silty-loam	4	1.0000	452	0.0000	0.00						
openwater	5	5–10	3	silty-loam	4	1.0000	453	0.0000	0.00						
openwater	5	>10	4	silty-loam	4	1.0000	454	0.0000	0.00						
crop	1	<0.5	1	loam	5	0.4000	511	0.0000	0.00						
crop	1	0.5–5	2	loam	5	0.4500	512	0.0000	0.00						
crop	1	5–10	3	loam	5	0.5000	513	0.0000	0.00						
crop	1	>10	4	loam	5	0.5500	514	0.0000	0.00						
grass	2	<0.5	1	loam	5	0.2000	521	0.0000	0.00						
grass	2	0.5–5	2	loam	5	0.2500	522	0.0000	0.00						
grass	2	5–10	3	loam	5	0.3000	523	0.0000	0.00						
grass	2	>10	4	loam	5	0.3500	524	0.0000	0.00						
forest	3	<0.5	1	loam	5	0.1000	531	0.0000	0.00						
forest	3	0.5–5	2	loam	5	0.1500	532	0.0000	0.00						
forest	3	5–10	3	loam	5	0.2000	533	0.0000	0.00						
forest	3	>10	4	loam	5	0.2500	534	0.0000	0.00						
bare soil	4	<0.5	1	loam	5	0.5000	541	0.0000	0.00						
bare soil	4	0.5–5	2	loam	5	0.5500	542	0.0000	0.00						
bare soil	4	5–10	3	loam	5	0.6000	543	0.0000	0.00						
bare soil	4	>10	4	loam	5	0.6500	544	0.0000	0.00						
openwater	5	<0.5	1	loam	5	1.0000	551	0.0000	0.00						
openwater	5	0.5–5	2	loam	5	1.0000	552	0.0000	0.00						
openwater	5	5–10	3	loam	5	1.0000	553	0.0000	0.00						
openwater	5	>10	4	loam	5	1.0000	554	0.0000	0.00						
crop	1	<0.5	1	sandyclaylo	7	0.4300	711	0.0000	0.00						
crop	1	0.5–5	2	sandyclaylo	7	0.4800	712	0.0000	0.00						
crop	1	5–10	3	sandyclaylo	7	0.5300	713	0.0000	0.00						
crop	1	>10	4	sandyclaylo	7	0.5800	714	0.0000	0.00						
grass	2	<0.5	1	sandyclaylo	7	0.2300	721	0.0000	0.00						
grass	2	0.5–5	2	sandyclaylo	7	0.2800	722	0.0000	0.00						
grass	2	5–10	3	sandyclaylo	7	0.3300	723	0.0000	0.00						
grass	2	>10	4	sandyclaylo	7	0.3800	724	0.0000	0.00						
forest	3	<0.5	1	sandyclaylo	7	0.1300	731	0.0000	0.00						
forest	3	0.5–5	2	sandyclaylo	7	0.1800	732	0.0000	0.00						
forest	3	5–10	3	sandyclaylo	7	0.2300	733	0.0000	0.00						
forest	3	>10	4	sandyclaylo	7	0.2800	734	0.0000	0.00						
bare soil	4	<0.5	1	sandyclaylo	7	0.5300	741	0.0000	0.00						
bare soil	4	0.5–5	2	sandyclaylo	7	0.5800	742	0.0000	0.00						
bare soil	4	5–10	3	sandyclaylo	7	0.6300	743	0.0000	0.00						
bare soil	4	>10	4	sandyclaylo	7	0.6800	744	0.0000	0.00						
openwater	5	<0.5	1	sandyclaylo	7	1.0000	751	0.0000	0.00						
openwater	5	0.5–5	2	sandyclaylo	7	1.0000	752	0.0000	0.00						
openwater	5	5–10	3	sandyclaylo	7	1.0000	753	0.0000	0.00						
openwater	5	>10	4	sandyclaylo	7	1.0000	754	0.0000	0.00						

Table A3. *Cont.*

LANDUSERO	LANDUSENUM	SLOPE_[%]	SLOPENUM	SOILTYPE	SOILNUM	RUNOFFCOEF	UNIQUE_NUM	SOIL_BARE	SLOPE_BARE	BAREROCOEF	UNIQUEBARE	NUM_IMP_RO	SLOPE_IMP	IMPROCOEF	UNIQUEIMP
crop	1	<0.5	1	clayloam	9	0.4800	911	0.0000	0.00						
crop	1	0.5–5	2	clayloam	9	0.5300	912	0.0000	0.00						
crop	1	5–10	3	clayloam	9	0.5800	913	0.0000	0.00						
crop	1	>10	4	clayloam	9	0.6300	914	0.0000	0.00						
grass	2	<0.5	1	clayloam	9	0.2800	921	0.0000	0.00						
grass	2	0.5–5	2	clayloam	9	0.3300	922	0.0000	0.00						
grass	2	5–10	3	clayloam	9	0.3800	923	0.0000	0.00						
grass	2	>10	4	clayloam	9	0.4300	924	0.0000	0.00						
forest	3	<0.5	1	clayloam	9	0.1800	931	0.0000	0.00						
forest	3	0.5–5	2	clayloam	9	0.2300	932	0.0000	0.00						
forest	3	5–10	3	clayloam	9	0.2800	933	0.0000	0.00						
forest	3	>10	4	clayloam	9	0.3300	934	0.0000	0.00						
bare soil	4	<0.5	1	clayloam	9	0.5800	941	0.0000	0.00						
bare soil	4	0.5–5	2	clayloam	9	0.6300	942	0.0000	0.00						
bare soil	4	5–10	3	clayloam	9	0.6800	943	0.0000	0.00						
bare soil	4	>10	4	clayloam	9	0.7300	944	0.0000	0.00						
openwater	5	<0.5	1	clayloam	9	1.0000	951	0.0000	0.00						
openwater	5	0.5–5	2	clayloam	9	1.0000	952	0.0000	0.00						
openwater	5	5–10	3	clayloam	9	1.0000	953	0.0000	0.00						
openwater	5	>10	4	clayloam	9	1.0000	954	0.0000	0.00						
crop	1	<0.5	1	clay	12	0.5500	1211	0.0000	0.00						
crop	1	0.5–5	2	clay	12	0.6000	1212	0.0000	0.00						
crop	1	5–10	3	clay	12	0.6500	1213	0.0000	0.00						
crop	1	>10	4	clay	12	0.7000	1214	0.0000	0.00						
grass	2	<0.5	1	clay	12	0.3500	1221	0.0000	0.00						
grass	2	0.5–5	2	clay	12	0.4000	1222	0.0000	0.00						
grass	2	5–10	3	clay	12	0.4500	1223	0.0000	0.00						
grass	2	>10	4	clay	12	0.5000	1224	0.0000	0.00						
forest	3	<0.5	1	clay	12	0.2500	1231	0.0000	0.00						
forest	3	0.5–5	2	clay	12	0.3000	1232	0.0000	0.00						
forest	3	5–10	3	clay	12	0.3500	1233	0.0000	0.00						
forest	3	>10	4	clay	12	0.4000	1234	0.0000	0.00						
bare soil	4	<0.5	1	clay	12	0.6500	1241	0.0000	0.00						
bare soil	4	0.5–5	2	clay	12	0.7000	1242	0.0000	0.00						
bare soil	4	5–10	3	clay	12	0.7500	1243	0.0000	0.00						
bare soil	4	>10	4	clay	12	0.8000	1244	0.0000	0.00						
openwater	5	<0.5	1	clay	12	1.0000	1251	0.0000	0.00						
openwater	5	0.5–5	2	clay	12	1.0000	1252	0.0000	0.00						
openwater	5	5–10	3	clay	12	1.0000	1253	0.0000	0.00						
openwater	5	>10	4	clay	12	1.0000	1254	0.0000	0.00						

Note: LANDUSERO: Runoff class for landuse; LANDUSENUM: Number of runoff class for landuse; SLOPE_[%]: Slope; SLOPENUM: Slope class; SOILTYPE: Soil type; SOILNUM: Soil class; RUNOFFCOEF: Runoff coefficient; UNIQUE_NUM: Unique Number ($100 \times$ SOILNUM $+ 10 \times$ LANDUSENUM $+ 1 \times$ SLOPENUM); SOIL_BARE: Soil type (bare); SLOPE_BARE: Slope class of bare soil; BARECOEF: Bare soil runoff coefficient; UNIQUEBARE: Unique Number ($10 \times$ SOIL_BARE $+ 1 \times$ SLOPE_BARE); IMPLUSERO: Impervious landuse runoff; NUM_IMP_RO: Impervious landuse runoff class; SLOPE_IMP: Slope class of impervious landuse type; IMROCOEF: Runoff coefficient for impervious landuse type; UNIQUEIMP: Unique Number ($10 \times$ NUM_IMP_RO $+ 1 \times$ SLOPE_IMP).

Table A4. The location of monitoring points.

Monitoringpoints	Location	Latitude Andlongitude	Groundwaterdepth (m)	Δ*h*(m)
0	Qingyang village in Pinggu district	40°6′5.09″ N, 117°4′6.10″ E	25.32	1.71
1	Chenjiaying village in Chengguan town ofYanqing country	40°27′25.34″ N, 116°2′8.10″ E	13.97	11.8
2	Xiyangfang village in Lejiabao of Yanqingcountry	40°31′6.05″ N, 115°55′7.34″ E	13.70	1.08
3	Xiaonanyuan in Yongning town of Yanqingcountry	40°31′41.67″ N, 116°9′48.53″ E	9.84	1.7
4	Shahe village in Chengguan town of Miyuncountry	40°23′34.24″ N, 116°51′8.85″ E	26.91	3.18
5	Menlou village in Pinggu district	40°4′42.10″ N, 117°3′28.42″ E	1.77	3.95
6	Tianjiaying in Shunyi district	40°6′31.43″ N, 116°48′12.30″ E	14.72	1.66
7	Changziying in Daxing district	39°41′14.73″ N, 116°35′11.77″ E	4.55	4.32
8	Xiaotangshan village in Xiaotangshan town ofChangping district	40°10′14.03″ N, 116°22′41.83″ E	2.21	5.25
9	Yangzhenerjie in Shunyi district	40°9′0.43″ N, 116°49′39.30″ E	2.48	1.63
10	Henan village in Shunyi district	40°6′14.31″ N, 116°42′12.80″ E	6.47	8.74
11	Nanhuofa in Tongzhou district	39°47′56.62″ N, 116°39′46.09″ E	2.43	2.51
12	Dongran village in Haidian district	39°57′15.85″ N, 116°16′14.79″ E	30.31	3.95
13	Tsinghua University in Haidian district	39°59′58.80″ N, 116°19′35.20″ E	31.07	4.82
14	Peking University in Haidian district	39°59′12.82″ N, 116°18′21.04″ E	25.54	5.03
15	Dahongmen in Fengtai district	39°49′40.13″ N, 116°25′5.79″ E	23.91	0.53
16	Baliqiao village in Chaoyang district	39°54′35.61″ N, 116°36′55.99″ E	58.77	2.79
17	Working people's Cultural Palace in Dongchengdistrict	39°54′38.35″ N, 116°24′0.57″ E	27.47	1.49
18	Xingli village in Fangshan district	39°35′49.64″ N, 116°4′59.75E	5.05	9.16
19	Liangxiang Development Zone in Fangshandistrict	39°42′28.84″ N, 116°12′16.75″ E	16.68	5.57
20	Lizhuang village in Fangshan district	39°35′56.17″ N, 116°0′27.92″ E	8.45	9.18
21	Capital Normal University in Haidian district	39°55′49.09″ N, 116°18′27.63″ E	32.49	2.21
22	Tiantan Park	39°53′1.39″ N, 116°24′45.93″ E	28.44	1.1
23	Dingfu village of Chaoyang district	39°55′7.42″ N, 116°33′59.34″ E	2.93	1.5
24	Luhe middle school in Tongzhou district	39°53′56.82″ N, 116°39′23.63″ E	15.87	5.13
25	Water source plant in Fengtai district	39°51′49.68″ N, 116°19′6.05″ E	24.22	2.5
26	Yuquan mountain in Haidian district	39°59′38.15″ N, 116°14′52.83″ E	33.03	7.62

Note: Groundwater depth and water level variation (Δ*h*) is the annual average values.

References

1. Han, D.; Currell, M.J.; Cao, G.; Hall, B. Alterations to groundwater recharge due to anthropogenic landscape change. *J. Hydrol.* **2017**, *554*, 545–557. [CrossRef]
2. Yang, Y.; Lerner, D.N.; Barrett, M.H.; Tellam, J.H. Quantification of groundwater recharge in the city of Nottingham, UK. *Environ. Geol.* **1999**, *38*, 183–198. [CrossRef]
3. Liu, Y.; Gebremeskel, S.; Smedt, F.D.; Hoffmann, L. Predicting storm runoff from different land-use classes using a geographical information systembased distributed model. *J. Hydrol.* **2006**, *20*, 533–548.
4. Dow, C.L.; DeWalle, D.R. Trends in evaporation and bowen ratio on urbanizing watersheds in eastern United States. *Water Resour. Res.* **2000**, *36*, 1835–1843. [CrossRef]
5. Larsen, T.A.; Hoffmann, S.; Lüthi, C.; Truffer, B.; Maurer, M. Emerging solutions to the water challenges of an urbanizing world. *Science* **2016**, *352*, 928–933. [CrossRef] [PubMed]
6. Zhou, L.; Dickinson, R.E.; Tian, Y.; Fang, J.; Li, Q.; Kaufmann, R.K.; Tucker, C.J.; Myneni, R.B. Evidence for a significant urbanization effect on climate in China. *Proc. Natl. Acad. Sci. USA* **2004**, *101*, 9540–9544. [CrossRef] [PubMed]
7. Fu, P. A time series analysis of urbanization induced land use and land cover change and its impact on land surface temperature with landsat imagery. *Remote Sens. Environ.* **2016**, *175*, 205–214. [CrossRef]
8. Su, S.; Ma, X.; Xiao, R. Agricultural landscape pattern changes in response to urbanization at ecoregional scale. *Ecol. Indic.* **2014**, *40*, 10–18. [CrossRef]
9. Tian, Y.; Jim, C.Y.; Wang, H. Assessing the landscape and ecological quality of urban green spaces in a compact city. *Landsc. Urban Plan.* **2014**, *121*, 97–108. [CrossRef]
10. Kadish, J.; Netusil, N. Valuing vegetation in an urban watershed. *Landsc. Urban Plan.* **2012**, *104*, 59–65. [CrossRef]
11. Davies, A.S.; Hernebring, C.; Svensson, G. The impacts of climate change and urbanisation on drainage in helsingborg, sweden: Suburban stormwater. *J. Hydrol.* **2008**, *350*, 114–125. [CrossRef]
12. Poelmans, L.; Rompaey, A.; Batelaan, O. Coupling urban expansion models and hydrological models: How important are spatial patterns? *Land Use Policy* **2010**, *27*, 965–975. [CrossRef]
13. Huang, T.; Li, X.; Rijnaarts, H.; Grotenhuis, T. Effects of storm runoff on the thermal regime and water quality of a deep, stratified reservoir in a temperate monsoon zone, in northwest China. *Sci. Total Environ.* **2014**, *485*, 820–827. [CrossRef] [PubMed]
14. Corbett, D.R.; Chanton, J.; Burnett, W.; Dillon, K.; Rutkowski, C.; Fourqurean, J.W. Patterns of groundwater discharge into Florida Bay. *Limnol. Oceanogr.* **1999**, *44*, 1045–1055. [CrossRef]
15. Rose, S.; Peters, N.E. Effects of urbanization on streamflow in the Atlanta area (Georgia, USA): A comparative hydrological approach. *Hydrol. Process.* **2001**, *15*, 1441–1457. [CrossRef]
16. Grischek, T.; Nestler, W.; Piechniczek, D.; Fischer, T. Urban groundwater in Dresden, Germany. *Hydrogeol. J.* **1996**, *4*, 48–63. [CrossRef]
17. Kalin, L.; Hantush, M.M. Hydrologic modeling of an eastern Pennsylvania watershed with NEXRAD and rain gauge data. *J. Hydrol. Eng.* **2006**, *11*, 555–569. [CrossRef]
18. Barron, O.V.; Donn, M.J.; Barr, A.D. Urbanisation and shallow groundwater: predicting changes in catchment hydrological responses. *Water Resour. Manag.* **2013**, *27*, 95–115. [CrossRef]
19. Zhang, D.; Madsen, H.; Ridler, M.E.; Refsgaard, J.C. Impact of uncertainty description on assimilating hydraulic head in the MIKE SHE distributed hydrological model. *Adv. Water Resour.* **2015**, *86*, 400–413. [CrossRef]
20. Gumindoga, W.; Rientjes, T.; Haile, A.; Dube, T. Predicting streamflow for land cover changes in the upper Gilgel Abay River basin, Ethiopia: A TOPMODEL based approach. *Phys. Chem. Earth* **2014**, *76*, 3–15. [CrossRef]
21. Singh, G.; Saraswat, D. Development and evaluation of targeted marginal land mapping approach in SWAT model for simulating water quality impacts of selected second generation biofeedstock. *Environ. Model. Softw.* **2016**, *81*, 26–39. [CrossRef]
22. Gebreyohannes, T.; Smedt, F.; Walraevens, K.; Gebresilassie, S. Application of a spatially distributed water balance model for assessing surface water and groundwater resources in the Geba basin, Tigray, Ethiopia. *J. Hydrol.* **2013**, *499*, 110–123. [CrossRef]

23. Batelaan, O.; Wang, Z.; de Smedt, F. An adaptive GIS toolbox for hydrological modelling. In *Application of Geographic Information Systems in Hydrology and Water Resources Management*; Kovar, K., Nachtnebel, H.P., Eds.; International Association of Hydrological Sciences: Wallingford, UK, 1996; pp. 3–9.

24. Moiwo, J.P.; Tao, F. Groundwater recharge and discharge analysis for Land use conditions suitable for the hydrology and ecology of semiarid regions. *Hydrol. Res.* **2014**, *45*, 563. [CrossRef]

25. Wang, Y.; Lei, X.; Liao, W.; Jiang, Y.; Huang, X.; Liu, J.; Song, X.; Wang, H. Monthly spatial distributed water resources assessment: A case study. *Comput. Geosci.* **2012**, *45*, 319–330. [CrossRef]

26. Zomlot, Z.; Verbeiren, B.; Huysmans, M.; Batelaan, O. Spatial distribution of groundwater recharge and base flow: Assessment of controlling factors. *J. Hydrol.* **2015**, *4*, 349–368. [CrossRef]

27. Zomlot, Z.; Verbeiren, B.; Huysmans, M.; Batelaan, O. Trajectory analysis of land use and land cover maps to improve spatial-temporal patterns, and impact assessment on groundwater recharge. *J. Hydrol.* **2017**, *554*, 558–569. [CrossRef]

28. Lin, L.; Yin, Y.; Xie, Y. Study on rainfall infiltration recharge under conditions of difference land use and cover in Songnen basin. *Water Resour. Hydropower Northeast* **2011**, *1*, 35–37. (In Chinese)

29. Dams, J.; Dujardin, J.; Reggers, R.; Bashir, I. Mapping impervious surface change from remote sensing for hydrological modeling. *J. Hydrol.* **2013**, *485*, 84–95. [CrossRef]

30. Jiang, Y.; Tian, F.; Luo, Y.; Wang, R. Research on the relationship between groundwater level and layered subsidence in typical regions of Beijing. *South-to-North Water Transf. Water Sci. Technol.* **2015**, *13*, 95–99. (In Chinese)

31. Bureau, B.S. *Beijing Statistical Yearbook 2010*; China Statistics Press: Beijing, China, 2010. (In Chinese)

32. Qiao, Z.; Tian, G.; Xiao, L. Diurnal and seasonal impacts of urbanization on the urban thermal environment: A case study of Beijing using MODIS data. *ISPRS J. Photogramm. Remote Sens.* **2013**, *85*, 93–107. [CrossRef]

33. Sun, Z.; Feng, S.; Yang, Z.; Wu, H. Primary analysis of the precipitation characteristics for Beijing during the period from 1950 to 2005. *J. Irrig. Drain.* **2007**, *26*, 12–16.

34. Pan, Y.; Zhu, L.; Du, L.; Xu, H. Estimation of rainfall infiltration in Beijing plain using WetSpass. *J. Water Resour. Res.* **2012**, *1*, 245–250. (In Chinese) [CrossRef]

35. Tong, Y.; Wang, Y. Dynamic simulation and policy analysis of Beijing population. *China Popul. Ressour. Environ.* **2016**, *26*, 170–176. (In Chinses)

36. Wang, J.; Yang, F.; He, B.; Zhao, L. Study on reducing shadow impact in the extraction impervious surface coverage of urban based on quickbird image. *Remote Sens. Inf.* **2008**, *3*, 69–73. (In Chinese)

37. Shen, Z.; Hou, X.; Li, W.; Aini, G.; Chen, L.; Gong, Y. Impact of landscape pattern at multiple spatial scales on water quality: A case study in a typical urbanised watershed in China. *Ecol. Indic.* **2015**, *48*, 417–427. [CrossRef]

38. Mcgarigal, K. *Fragstats: Spatial Pattern Analysis Software for Categorical Maps*; University of Massachusetts: Amherst, MA, USA, 2002.

39. Batelaan, O.; de Smedt, F. Wetspass: A flexible, GIS based, distributed recharge methodology for regional groundwater modelling. In *Impact of Human Activity on Groundwater Dynamics*; Gehrels, H., Peters, J., Leibundgut, C., Eds.; International Association of Hydrological Sciences: Wallingford, UK, 2001; pp. 11–17.

40. Park, C.; Seo, J.; Lee, J.; Ha, K.; Koo, M.H. A distributed water balance approach to groundwater recharge estimation for Jeju volcanic island, Korea. *Geosci. J.* **2014**, *18*, 193–207. [CrossRef]

41. Batelaan, O.; de Smedt, F. GIS-based recharge estimation by coupling surface-subsurface water balances. *J. Hydrol.* **2007**, *337*, 337–355. [CrossRef]

42. Armanuos, A.M.; Negm, A. Assessment of the variations of local parameters of Wetspass model: Case study Nile Delta aquifer. *Procedia Eng.* **2016**, *154*, 276–283. [CrossRef]

43. Batelaan, O.; Woldeamlak, S.T. *Arcview Interface for WetSpass, Version 13-06-2007*; Vrije University Brussels: Brussels, Belgium, 2007.

44. Gao, C. *China Groundwater Level Yearbook for Geo-Environmental Monitoring*; China Land Press: Beijing, China, 2013; p. 583. (In Chinese)

45. Xu, C.; Singh, V. Review on regional water resources assessment models under stationary and changing climate. *Water Resour. Manag.* **2004**, *18*, 591–612. [CrossRef]

46. Tahir, M.E.; Wang, W.; Xu, C.; Zhang, Y. Comparison of methods for estimation of regional actual evapotranspiration in data scarce regions: The Blue Nile region-Eastern Sudan. *J. Hydrol. Eng.* **2012**, *17*, 578–589. [CrossRef]

47. Fiquepron, J.; Garcia, S.; Stenger, A. Land use impact on water quality: Valuing forest services in terms of the water supply sector. *J. Environ. Manag.* **2013**, *126*, 13–21. [CrossRef] [PubMed]

48. Zhu, L.; Liu, C.; Li, X. Precipitation infiltration change in Beijing plain in the contex of urbanization. *Earth Sci.* **2013**, *38*, 1065–1072. (In Chinese)

49. Shuster, W.; Bonta, J.; Thurston, H.; Warnemuende, E.; Smith, E. Impacts of impervious surface on watershed hydrology: A review. *Urban Water J.* **2005**, *2*, 263–275. [CrossRef]

50. Tomer, M.D.; Schilling, K.E. A simple approach to distinguish land-use and climate-change effects on watershed hydrology. *J. Hydrol.* **2009**, *376*, 24–33. [CrossRef]

51. Wang, M.; Zhang, D.; Adhityan, A.; Ng, W.J.; Dong, J.; Tan, S.K. Assessing cost-effectiveness of bioretention on stormwater in response to climate change and urbanization for future scenarios. *J. Hydrol.* **2016**, *543*, 423–432. [CrossRef]

52. Melki, A.; Abdollahi, K.; Fatahi, R.; Abida, H. Groundwater recharge estimation under semi arid climate: Case of Northern Gafsa watershed, Tunisia. *J. Afr. Earth Sci.* **2017**, *132*, 37–46. [CrossRef]

53. Shrestha, S.; Bach, T.V.; Pandey, V.P. Climate change impacts on groundwater resources in Mekong Delta under representative concentration pathways (RCPs) scenarios. *Environ. Sci. Policy* **2016**, *61*, 1–13. [CrossRef]

54. Jia, Y.W.; Zhao, H.L.; Niu, C.W.; Jiang, Y.Z.; Hong, G.; Zhi, X.; Zhao, X.L.; Zhao, Z.X. A WebGIS-based system for rainfall-runoff prediction and real-time water resources assessment for Beijing. *Comput. Geosci.* **2009**, *35*, 1517–1528. [CrossRef]

55. Minnig, M.; Moeck, C.; Radny, D.; Schirmer, M. Impact of urbanization on groundwater recharge rates in Dübendorf, Switzerland. *J. Hydrol.* **2017**, in press. [CrossRef]

56. Chen, Q.; Wang, L.; Yuan, L. Analysis of urban landscape pattern change in Yanzhou city based on TM/ETM images. *Procedia Earth Planet. Sci.* **2009**, *1*, 1191–1197. [CrossRef]

57. Ji, D.; Wen, Y.; Wei, J.; Wu, Z. Relationships between landscape spatial characteristics and surface water quality in the Liu Xi River watershed. *Acta Ecol. Sinica* **2015**, *35*, 246–253. (In Chinese)

58. Li, J.; Zhou, Z.X. Coupled analysis on landscape pattern and hydrological processes in Yanhe watershed of China. *Sci. Total Environ.* **2015**, *505*, 927–938. [CrossRef] [PubMed]

59. Jia, H.; Ma, H.; Wei, M. Urban wetland planning: A case study in the Beijing central region. *Ecol. Complex.* **2011**, *8*, 213–221. [CrossRef]